

Fabrication, microstructure and laser performance of Yb³⁺ doped CaF₂-YF₃ transparent ceramics



Weiwei Li^a, Haijun Huang^b, Bingchu Mei^{a,*}, Cong Wang^{c,d}, Jie Liu^{c,d,**}, Shaozhao Wang^a, Dapeng Jiang^{e,f}, Liangbi Su^{e,f,***}

^a State Key Laboratory of Advanced Technology for Materials Synthesis and Processing, Wuhan University of Technology, Wuhan, 430070, China

^b School of Science, Wuhan University of Technology, Wuhan, 430070, China

^c Shandong Provincial Key Laboratory of Optics and Photonic Devices, School of Physics and Electronics, Shandong Normal University, Jinan, 250014, China

^d Institute of Data Science and Technology, Shandong Normal University, Jinan, 250014, China

^e Shanghai Institute of Ceramics, Synthetic Single Crystal Research Center, Chinese Academy of Sciences, Shanghai, 201800, China

^f Shanghai Institute of Ceramics, Key Laboratory of Transparent and Opto-functional Inorganic Materials, Chinese Academy of Sciences, Shanghai, 201800, China

ARTICLE INFO

Keywords:

Yb³⁺: CaF₂
Buffer ions
Optical properties
Laser performance
Microstructure

ABSTRACT

Yb³⁺: CaF₂ transparent ceramics are promising laser gain medium with outstanding performance. Considering Yb³⁺ ions tend to form clusters in CaF₂ host, the aim of this paper was to investigate the influence of Y³⁺ ions doping on the spectroscopic properties of 3 at.% Yb³⁺: CaF₂ transparent ceramics. High optical quality of Yb³⁺: CaF₂-YF₃ samples doped with different Y³⁺ ions concentrations (from 1 at.% to 6 at.%) were fabricated by hot-pressed (HP) method. The effect of Y³⁺ ions on the crystal structure, morphology of the particles and microstructure of the ceramics were studied. Interestingly, the particle size of Yb³⁺: CaF₂ powders decreased with the increasing of Y³⁺ ions concentrations, while the emission intensity at 1028 nm and lifetime first increased then decreased. Continuous-wave (CW) laser at the wavelength of 1049 nm was obtained in 3 at.% Yb³⁺, 1 at.% Y³⁺: CaF₂ ceramics. The maximum output power was 1.16 W with a slope efficiency of 29.3%. To the best of our knowledge, this is the first demonstration of laser in Yb³⁺: CaF₂-YF₃ ceramics.

1. Introduction

Transparent ceramics is used as laser gain medium due to their excellent properties, such as easy fabrication process, low fabrication cost and high doping concentration [1,2]. Laser ceramics, such as calcium fluoride (CaF₂), own wide transparency wavelength range (from 0.125 to 9 μm), low phonon energy (350 cm⁻¹) and refractive index (1.428 at 1.064 μm). These characterizations are important when these materials are being taken into consideration for application in high power laser system.

Among all the rare-earth ions, Yb³⁺ is a very attractive ion because it has a simple electronic structure, no intrinsic process of concentration quenching, long lifetime, and broad emission spectra [3,4]. These special features make Yb³⁺ very suitable for ultra-short laser and high-power laser applications [5–7]. However, rare-earth ions, such as Yb³⁺,

Nd³⁺ and Tm³⁺, easily form the cluster structure in CaF₂ host even in low doping concentrations, which will degrade the luminescent properties and quantum efficiency. Hence, buffer ions (i.e. Na⁺, Y³⁺, La³⁺ and Gd³⁺ ion) have been introduced to CaF₂ single crystals to manipulate spectroscopic properties, such as Yb, Y: CaF₂ [8,9], Yb, Na: CaF₂ [10–12]. So far, most of the research work on tuning the spectral properties has been carried out on single crystal. There has been little investigation on the effect of buffer ions on the laser properties of Yb³⁺: CaF₂ transparent ceramics. Shotaro Kitajima et al. mixed three types of fluoride nanocrystal particles as sintering materials and fabricated Yb³⁺: CaF₂-LaF₃ transparent ceramics by hot isostatic pressing (HIP) method [13]. This paper proved that the formation of Yb²⁺ ions reduced and the laser efficiency enhanced after doped with La³⁺ ion.

It is well known that powders quality, phase composition and porosity amount play important roles in determining the optical quality of

* Corresponding author.

** Corresponding author. Shandong Provincial Key Laboratory of Optics and Photonic Devices, School of Physics and Electronics, Shandong Normal University, Jinan, 250014, China

*** Corresponding author. Shanghai Institute of Ceramics, Synthetic Single Crystal Research Center, Chinese Academy of Sciences, Shanghai, 201800, China. suliangbi@mail.sic.ac.cn

E-mail addresses: bmeilab@163.com (B. Mei), jieliu@sdu.edu.cn (J. Liu).

<https://doi.org/10.1016/j.ceramint.2020.05.003>

Received 18 March 2020; Received in revised form 28 April 2020; Accepted 1 May 2020

Available online 07 May 2020

0272-8842/ © 2020 Elsevier Ltd and Techna Group S.r.l. All rights reserved.

the laser ceramics. For these reasons, the porosity in the ceramics should be minimized as much as possible to diminish the scattering centers during the densification process. HP method is based on sintering nanoparticles at optimum temperatures accompanied by applying pressure on the mold. Therefore, the obtained green-body (usually ceramics and alloys) can be very dense. In fact, HP method is another technique to fabricate the rare-earth doped fluoride-based transparent ceramics except for the HIP method [14–17]. In 1964, the first Dy: CaF₂ ceramic laser in the world was fabricated by hot-pressed method [18]. Besides, the first laser generation of 3 at.% Yb³⁺: CaF₂ ceramics were also demonstrated by this method in 2013 [19]. Therefore, HP method is an efficient technique to fabricate CaF₂ transparent ceramics using nanoparticles as sintering powders.

Since Y³⁺ ions as buffer ions has been introduced to Nd³⁺: CaF₂ laser materials (including single crystal and ceramics) and achieve interesting results, a new Yb³⁺: CaF₂-YF₃ transparent ceramics was fabricated by HP method in this paper. The effect of Y³⁺ ion doping concentrations on the crystal structure, morphology of the particles, microstructure and spectral properties of Yb³⁺: CaF₂-YF₃ ceramics was studied. A maximum output power of 1.16 W with a slope efficiency of 29.3% was demonstrated for 3 at.% Yb³⁺, 1 at.%Y³⁺: CaF₂ sample. To the best of our knowledge, the laser performance of Yb³⁺: CaF₂-YF₃ ceramics has been demonstrated for the first time.

2. Experimental

In this paper, co-precipitation method was employed to synthesize a series of CaF₂: 3 at.% Yb³⁺, x at.% Y³⁺ (x = 0, 1, 3, 6) nanoparticles. High purity of commercial chemical reagent was used in this experiment, including calcium nitrate hydrate (99.9%, Sinopharm), ytterbium (III) nitrate hydrate (99.99%, Alfa Aesar), yttrium nitrate hydrate (99.99%, Sigma-Aldrich) and potassium fluoride hydrate (99.9% purity, Sinopharm). The details of the powders synthesized process were according to our previous report [20]. Stoichiometric amounts of Ca(NO₃)₂·4H₂O, Yb(NO₃)₃·5H₂O and Y(NO₃)₃·4H₂O were first dissolved in 64 ml distilled water together, and KF·2H₂O were also dissolved in 128 ml distilled water. Then, the solution of KF was dropped wise to the solution of Ca(NO₃)₂·4H₂O, Yb(NO₃)₃·5H₂O and Y(NO₃)₃·4H₂O under magnetic stirring. The mixture was centrifuged for 30 min at the speed of 11,000 rpm. The obtained gel was washed with distilled water four times to remove the residual ions of NO₃⁻ and K⁺. The powders were stored at -10 °C for 12 h before freeze-dried then dried in a freeze dryer (Scientz-12 N, Ningbo Scientz Biotechnology company, China) under the pressure of 1 Pa for 12 h. The dried powders were then milled manually in an agate mortar and spooned into the graphite mold. All the samples were sintered at the same temperature of 800 °C under the pressure of 40 MPa. Finally, both surfaces of the samples were mirror-polished by diamond slurries for the optical test.

Phase identification of the synthesized Yb³⁺: CaF₂-YF₃ powders was performed by the X-ray diffractometer (D/Max-RB, Rigaku, Japan). Hitachi U8010 microscope equipped with an Oxford energy dispersive X-ray (EDX) spectrum was used to analyze the particle size of the Yb³⁺: CaF₂-YF₃ powders, fracture microstructure and elemental analysis of the ceramics. PerkinElmer Lambda 750 UV-vis-IR spectrophotometer was used to record the in-line transmittance and the absorption curves of the Yb³⁺: CaF₂ transparent ceramics. The emission spectra and lifetime of the ceramics was measured on an Edinburgh FLS1000 spectrofluorometer. The emission signals were recorded with a NIR PMT (R5509-73, Hamamatsu).

3. Results and discussion

Fig. 1 (a) shows the powder X-ray diffraction patterns of 3 at.% Yb³⁺: CaF₂ nanopowders combined with 3 at.% Yb³⁺, x at.%Y³⁺: CaF₂ nanopowders, where x = 1, 3 and 6. From the XRD patterns, we can conclude that all the peak positions of the synthesized powders are

consistent with the Joint Committee on JCPDS card No. 65–0535. None of the peaks referred to Y³⁺, Yb³⁺ or other impurity phases were detected even after total doping concentration reached 9 at.%, suggesting that Yb³⁺ and Y³⁺ ions were successfully incorporated into the CaF₂ structure.

Fig. 1 (b) is the magnified view for the comparison of the (111) peak for the different concentrations of Y³⁺ ions. It can be observed that the diffraction peaks systematically shift towards the low angle along with the Y³⁺ increasing from 1 at.% to 6 at.%. This extent of diffraction peaks shifting enlarged upon the increasing of Y³⁺ doping concentration, implied that the unit cell parameters of CaF₂ host increased. The lattice parameters obtained from the structure refinement were about 5.4759 Å, 5.4783 Å, 5.4807 Å and 5.4890 Å. There might be two reasons for the increased lattice parameter: firstly, substitution of Ca²⁺ ion by trivalent Yb³⁺ and Y³⁺ ions need extra F⁻ ions as charge-compensators to the CaF₂ structure, the electronic repulsion between F⁻ ions leads to the expansion of the lattice parameter. Secondly, the small particle size of Yb³⁺: CaF₂-YF₃ powders increased the surface area of the particles, which resulted in surface tension and lattice expansion.

The average crystallite size (L) of the Yb³⁺: CaF₂-YF₃ nanoparticles was estimated using the Williamson-Hall equation [21]:

$$\beta_{hkl} \cos \theta = \frac{k\lambda}{L} + 4\epsilon \sin \theta$$

Here L is the crystallite size, ϵ is the macro strain presented in the Yb³⁺: CaF₂-YF₃ nanoparticles, θ represents the peak position, β_{hkl} represents the peak width of the diffraction peaks at half-maximum intensity, λ equal to 0.15406 nm and k equal to 0.89. The average sizes of 3 at.% Yb, 3 at.% Yb-1 at.% Y, 3 at.% Yb-3 at.% Y and 3 at.% Yb-6 at.% Y: CaF₂ particles were about 30.8 nm, 25.7 nm, 23.8 nm and 21.1 nm, respectively. The ionic radii different between the Ca²⁺ (0.99 Å), Y³⁺ (0.89 Å) and Yb³⁺ (0.86 Å) interrupts the grain growth process and limits the grain boundary mobility, which in turn decrease the crystallite sizes of the Yb³⁺: CaF₂-YF₃ powders [22].

FSEM is measured to analyze the influence of Y³⁺ ions doping on the morphology and particle size of Yb³⁺: CaF₂-YF₃ nanoparticles, as shown in Fig. 2. The FSEM images reveals that all the powders consisted of small agglomerated spherical-shaped particles. The doping of Y³⁺ ions did not change the morphology of the powders, but decreased the particle size of the powders. The particle sizes of the 3 at.% Yb, 3 at.% Yb-1 at.% Y, 3 at.% Yb-3 at.% Y and 3 at.% Yb-6 at.% Y: CaF₂ powders were about 37 nm, 33 nm, 31 nm and 28 nm. Besides, the particle size distribution became more uniform after doping with Y³⁺ ion. The result that doping with Y³⁺ ions could reduce the particle size of CaF₂ powders agreed with our previous studies [20]. It is particularly well known that the spherical shaped particle combined with the agglomeration, surface area and the sequence of pressing stages are important because the sintering ability depends upon these significant factors [23–25]. This means that the Yb³⁺: CaF₂-YF₃ nanopowders synthesized by co-preparation method is very suitable for HP sintering.

The sintered Yb³⁺: CaF₂-YF₃ transparent ceramics with thickness of 3.5 mm are presented in Fig. 3. All the ceramics sintered at 800 °C showed good optical quality except 3 at.%Yb³⁺, 6 at.%Y³⁺: CaF₂ sample. From the FSEM images, it could be concluded that the origin nanoparticle size of the 3 at.% Yb³⁺, 6 at.% Y³⁺: CaF₂ powders was smaller than other powders, but all the green bodies were sintered at the same temperature for comparison. Therefore, the sintering temperature of 800 °C may be a little high for the 3 at.% Yb³⁺, 6 at.% Y³⁺: CaF₂ powders. According, 800 °C is the optimized sintering temperature for the low concentration (possibly lower than 7 at.%) doped CaF₂ powders, but not suitable for the high doping concentration rare-earth doped CaF₂ transparent ceramics. The sintering parameter of HP method must be adjusted to match the different particle sizes of the powders, and this part of work is in progress.

The in-line transmittance curves of Yb³⁺: CaF₂-YF₃ transparent ceramics sintered at 800 °C are shown in Fig. 4. It can be seen that the

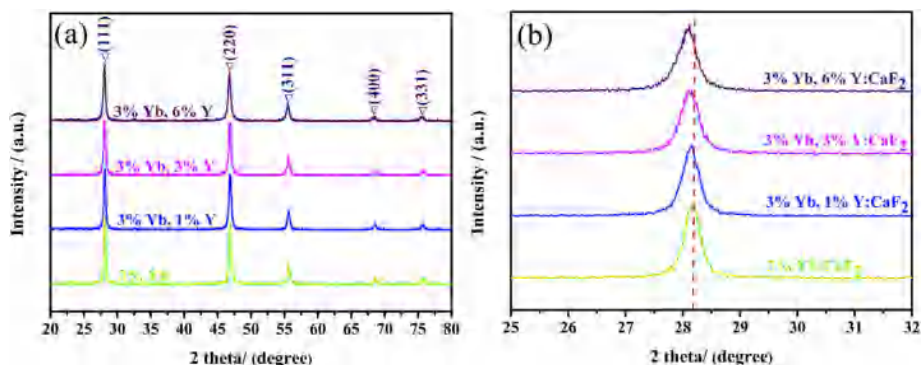


Fig. 1. (a) XRD patterns of $\text{Yb}^{3+}:\text{CaF}_2\text{-YF}_3$ nanoparticles, (b) the magnified view of (111) diffraction peak.

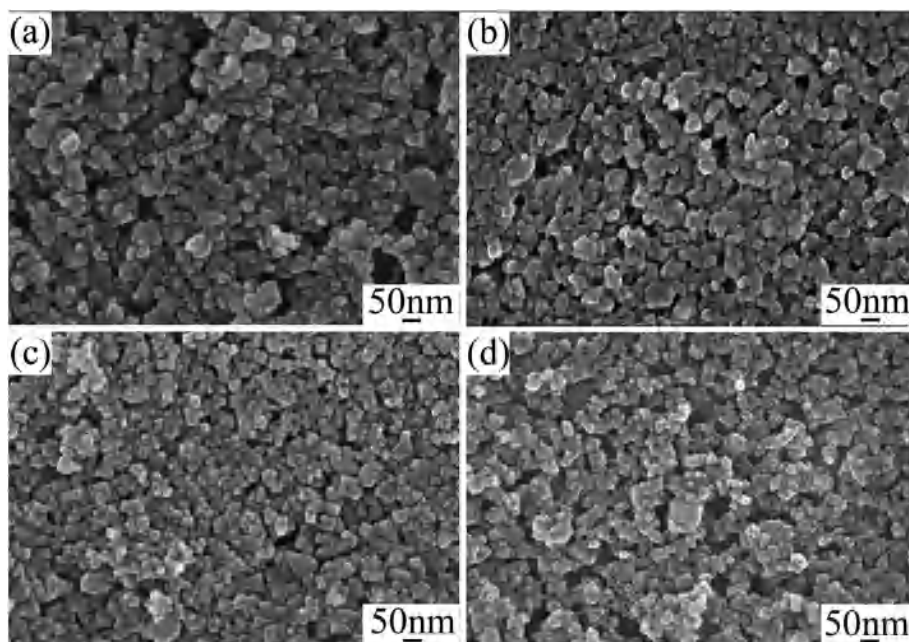


Fig. 2. FESM images of $\text{Yb}^{3+}:\text{CaF}_2\text{-YF}_3$ nanoparticles: (a) 3 at. % Yb, (b) 3 at. % Yb, 1 at. % Y, (c) 3 at. % Yb, 3 at. % Y and (d) 3 at. % Yb, 6 at. % Y.

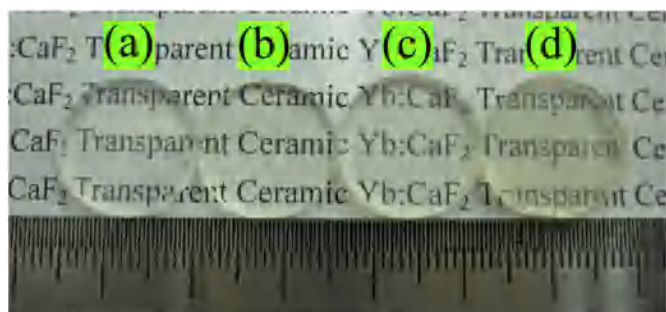


Fig. 3. Pictures of the polished $\text{Yb}^{3+}:\text{CaF}_2\text{-YF}_3$ transparent ceramic pellet: 3 at. % Yb, (b) 3 at. % Yb, 1 at. % Y, (c) 3 at. % Yb, 3 at. % Y and (d) 3 at. % Yb, 6 at. % Y.

transmittance of all the samples decreases in the short wavelength. The discrepancy between the samples in the transmittance was caused by the different polishing surfaces. 3 at. % Yb: CaF_2 ceramics had the highest transmittance among all the samples, the corresponding in-line transmittances at the wavelength of 400 nm and 1200 nm were 59.8% and 87.8%, respectively. There was still a gap between the measured transmittance and the theoretical value, but fortunately the transmittance of $\text{Yb}^{3+}:\text{CaF}_2\text{-YF}_3$ transparent ceramics could be greatly

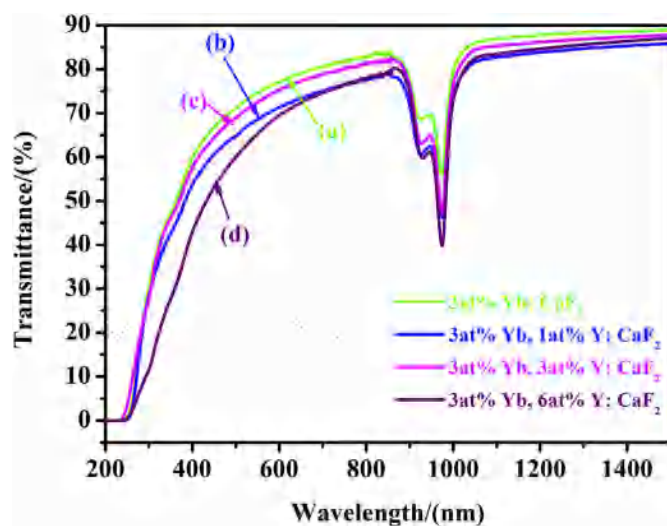


Fig. 4. Transmittance curves of $\text{Yb}^{3+}:\text{CaF}_2\text{-YF}_3$ ceramic samples ($\varnothing 16\text{ mm} \times 3.5\text{ mm}$).

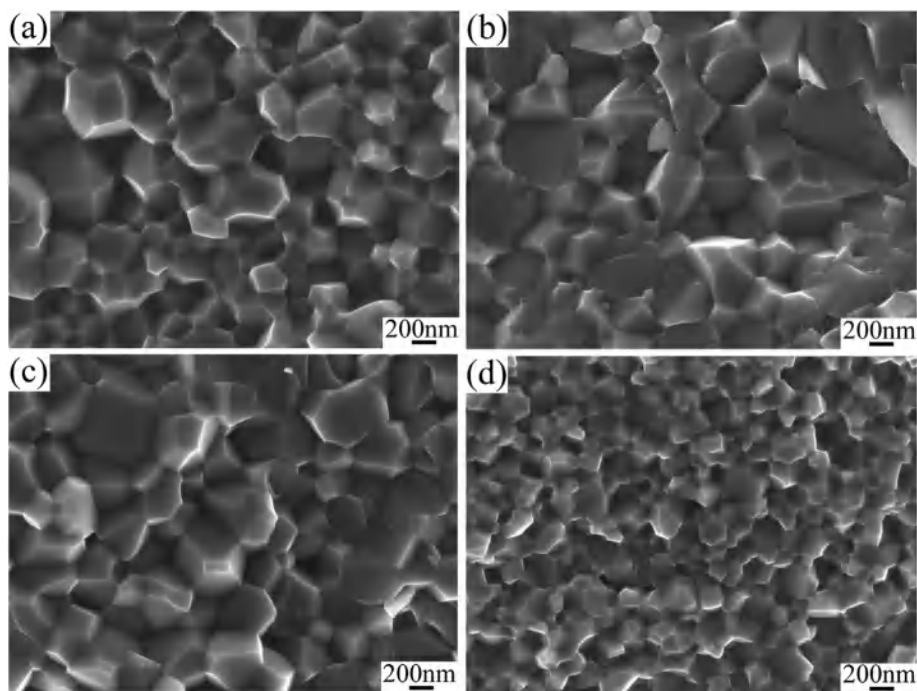


Fig. 5. FSEM images of $\text{Yb}^{3+}:\text{CaF}_2\text{-YF}_3$ transparent ceramic fracture surface: (a) 3 at. % Yb, (b) 3 at. % Yb, 1 at. % Y, (c) 3 at. % Yb, 3 at. % Y and (d) 3 at. % Yb, 6 at. % Y.

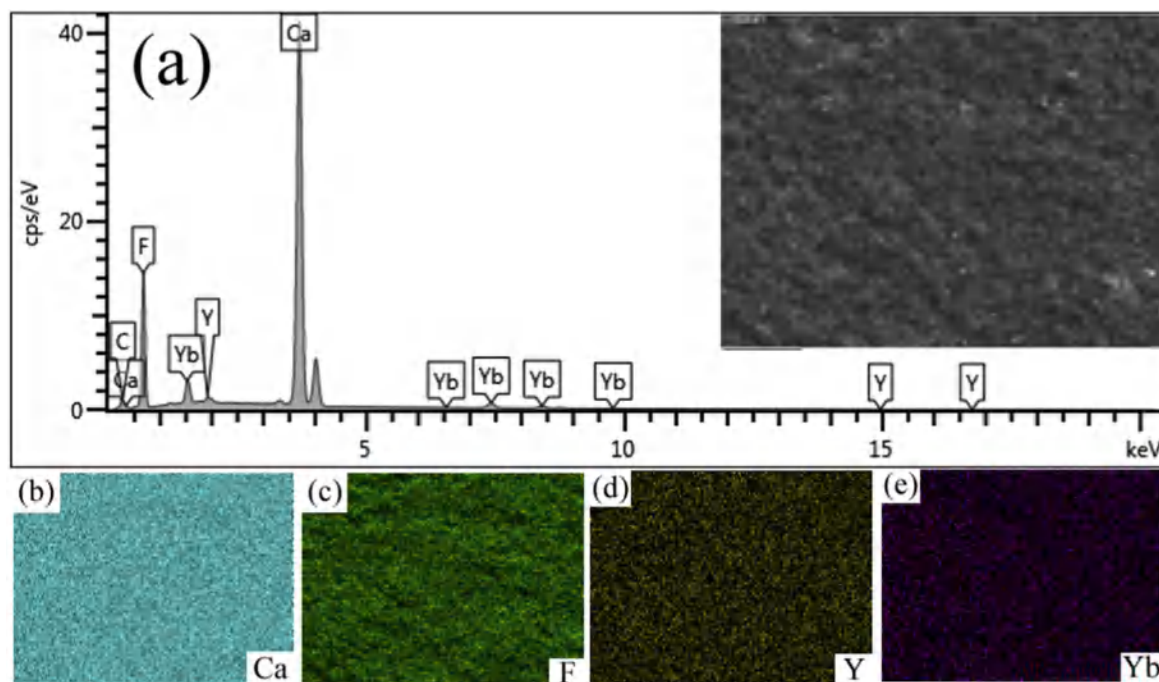


Fig. 6. (a) EDX spectrum and element mapping of (b) Ca, (c) F, (d) Y and (e) Yb of $\text{Yb}^{3+}:\text{CaF}_2\text{-YF}_3$ transparent ceramics.

increased after laser-graded polishing.

Fig. 5 shows the fracture microstructure of the $\text{Yb}^{3+}:\text{CaF}_2\text{-YF}_3$ transparent ceramics. The microstructure of all the samples were very dense and no obvious pores could be seen in the fracture surface. The average grain size of the 3 at.% Yb, 3 at.% Yb-1 at.% Y, 3 at.% Yb-3 at.% Y and 3 at.% Yb-6 at.% Y: CaF_2 samples calculated by the linear intercept method [26] were about 462 nm, 489 nm, 287 nm and 235 nm, respectively. Compared with the grain size ceramics fabricate by HIP method, such as 3–4 μm for the $\text{Yb}^{3+}:\text{CaF}_2\text{-LaF}_3$ [13] and 5–200 μm for the $\text{Nd}^{3+}:\text{CaF}_3$ ceramics [27], it is obvious that the grain size of

the $\text{Yb}^{3+}:\text{CaF}_2\text{-YF}_3$ transparent ceramics obtained by HP method is much smaller. The small grain size is beneficial to improving the mechanical properties of fluoride-based transparent ceramics, eventually achieve higher power laser output under the same optical quality. This is an advantage of HP method to prepare the rare-earth doped CaF_2 transparent ceramics.

The chemical composition of the $\text{Yb}^{3+}:\text{CaF}_2\text{-YF}_3$ transparent ceramics with Y^{3+} concentration of 1 at.% were investigated by EDX spectrum and elemental mappings, as shown in Fig. 6. It confirmed that Ca, Yb, Y and F were present in the sample as expected and all the

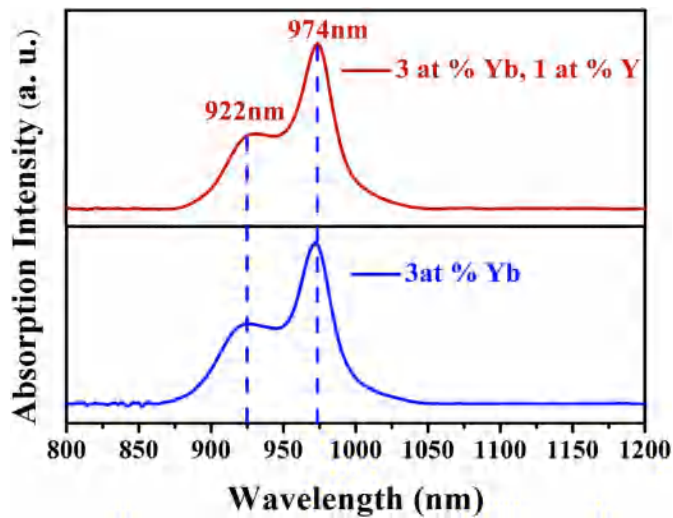


Fig. 7. Absorption spectra of 3 at.% Yb^{3+} and 3 at.% Yb^{3+} , 1 at.% Y^{3+} : CaF_2 ceramics.

elements were homogeneous in the ceramics. The EDX results also confirmed that the Yb and Y ions were successfully incorporated into the CaF_2 lattices.

The absorption coefficient of the 3 at.% Yb^{3+} and 3 at.% Yb^{3+} , 1 at.% Y^{3+} : CaF_2 transparent ceramics at room temperature is shown in Fig. 7. We can see that there are two absorption peaks located at 974 nm and 922 nm, corresponding to the transitions between ${}^2\text{F}_{7/2}$ and ${}^2\text{F}_{5/2}$. All the ceramics presented a broad absorption line around 974 nm with full width at half maximum (FWHM), making it appropriate for direct pumping by a high-power InGaAs laser diode (LD).

According to the absorption curves, the re-absorption at the wavelength between 900 nm to 1100 nm is very serious, so the excited wavelength has been settled at 896 nm. The emission spectra of the Yb^{3+} : $\text{CaF}_2\text{-YF}_3$ transparent ceramics doped with different Y^{3+} doping

concentrations excited with the xenon lamp at room temperature are shown in Fig. 8. The fluorescence spectra of all the samples presented broad emission band from 950 nm up to 1050 nm, which was promising beneficial to realize ultra-short laser pulses. There were four emission peaks located at 965 nm, 977 nm, 1011 nm and 1028 nm in the spectra curves. It was noted that the emission peaks of 965 nm and 977 nm existed in all the samples and the peak of 977 nm was the most dominant among all the emission bands, corresponding to zero phonon emission of Yb^{3+} ions. Besides, the intensity of emission peak at 1028 nm was enhanced after co-doped with 1 at.% Y^{3+} ions, then decreased when the Y^{3+} ions doping concentration further increased to 3 at.%. The emission intensity of the 3 at.% Yb, 6 at.% Y: CaF_2 transparent ceramics at 1011 nm was higher than that of 1028 nm.

The decay curves of Yb^{3+} : $\text{CaF}_2\text{-YF}_3$ transparent ceramics with different concentrations of Y^{3+} ions excited at the wavelength of 896 nm and monitored at 1028 nm are shown in Fig. 9. The decay curves were fitted with a single exponential function,

$$I(t) = I_0 + A\exp(-t/\tau)$$

Where $I(t)$ and I_0 are the initial intensity at $t = t$ and $t = 0$, respectively. A is a constant, t is the time and τ is the decay lifetimes. Using the above equation, the lifetime values for the 3 at.% Yb, 3 at.% Yb-1 at.% Y, 3 at.% Yb-3 at.% Y and 3 at.% Yb-6 at.% Y: CaF_2 transparent ceramics were calculated to be 5.2 ms, 6.3 ms, 5.8 ms and 4.6 ms. The lifetime increased first and decreased later with the increasing of Y^{3+} ions concentration. The dependence of decay lifetime on Y^{3+} ions concentration was in good accordance with the result of the luminescence intensity. It is particularly well known that longer emission lifetimes imply higher fluorescence quantum efficiency. Considering the emission spectra and lifetime results, it could be inferred that the doping with Y^{3+} ions prevent the formation of Yb^{3+} ions cluster structure and the optimal concentration of Y^{3+} ions in Yb^{3+} : CaF_2 might be about 1 at.%. As the optimum proportion of Yb: Y is about 3:1, the 3 at.% Yb, 1 at.% Y: CaF_2 transparent ceramics was chosen as a laser gain medium for

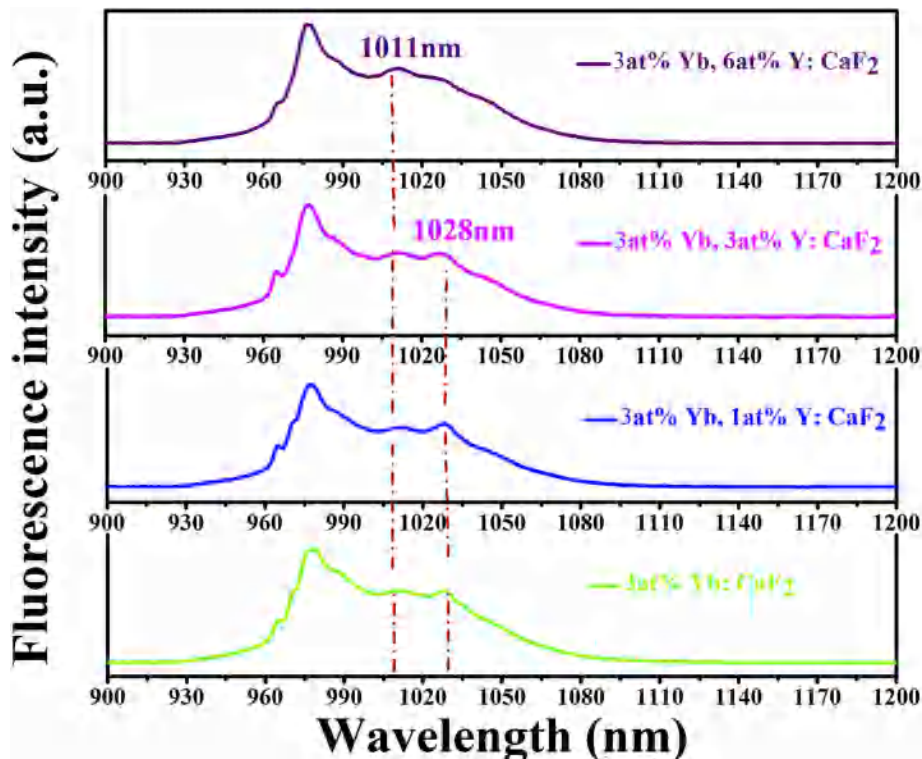


Fig. 8. Different Y^{3+} ions content emission spectra of the Yb^{3+} : $\text{CaF}_2\text{-YF}_3$ transparent ceramics ($\lambda_{\text{ex}} = 896$ nm).

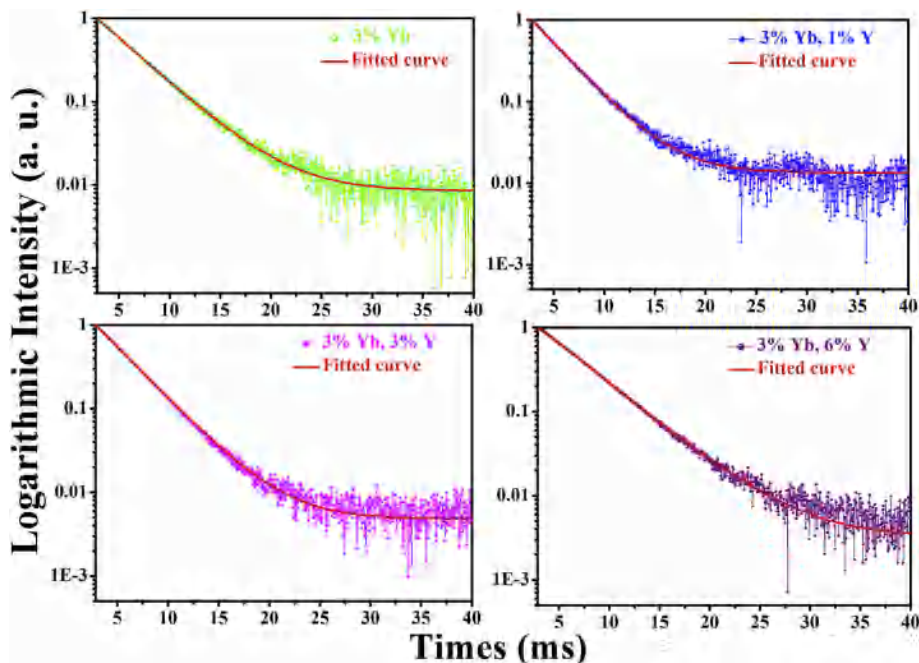


Fig. 9. Decay curves of the Yb^{3+} : $\text{CaF}_2\text{-YF}_3$ transparent ceramics under 986 nm excitation as a function of Y^{3+} ions.

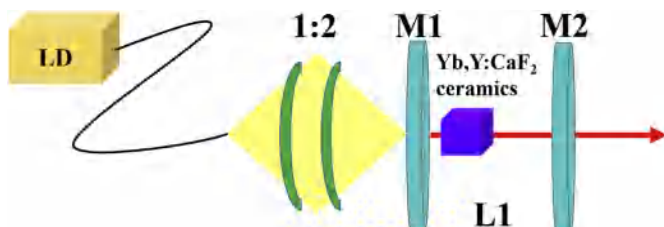


Fig. 10. Schematic diagram of the experimental setup.

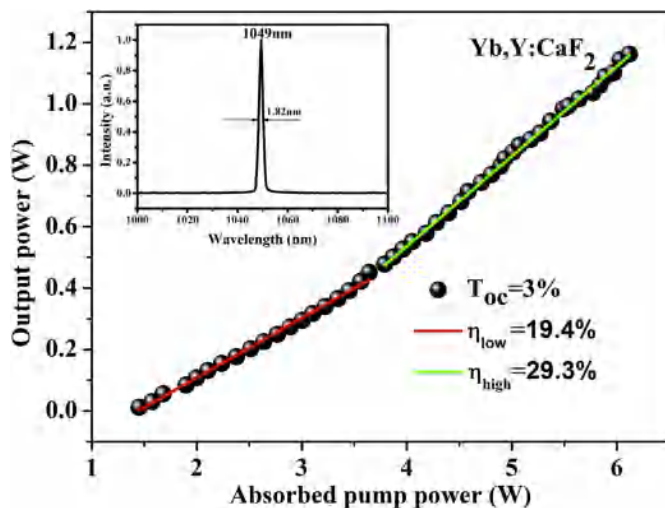


Fig. 11. Output power of Yb^{3+} : $\text{CaF}_2\text{-YF}_3$ transparent ceramics as a function of absorbed pump power, represent the slope efficiency.

laser experiment. The schematic diagram of the experimental setup is shown in Fig. 10. After laser grade polishing, the specimen was cut into $3 \text{ mm} \times 3 \text{ mm} \times 3 \text{ mm}$. The pump laser is a fiber-coupled laser diode temperature-tuned to 976 nm emission wavelength with a fiber core of $105 \mu\text{m}$ and numerical aperture of 0.22. The pump beam was focused on the ceramics by a 1:2 coupling system. The uncoated Yb^{3+} : $\text{CaF}_2\text{-YF}_3$ transparent ceramics were mounted in a copper block with water-

cooled to 12°C . The laser cavity was formed by an input mirror M1 (flat mirror) and an output coupler ($T_{\text{oc}} = 3\%$). The radius of curvature of the output coupler is 200 mm. Arm length L1 between M1 and M2 is 192 mm.

The continuous-wavelength (CW) output of 3 at.% Yb, 1 at.% Y: CaF_2 transparent ceramics as a function of absorbed pump power is shown in Fig. 11. The absorbed pump power for reaching laser thresholds of the sample was 1.45 W. Maximum output power of 1.16 W was obtained for the 3 at.% Yb, 1 at.% Y: CaF_2 transparent ceramics when the absorbed pump power was 6.12 W for $T_{\text{oc}} = 3\%$. The slope efficiency could be divided into two parts, the slope efficiency was 19.4% before the absorption pump power reaches 3.641 W and increased to 29.3% subsequently. The laser emitting spectrum of Yb^{3+} : $\text{CaF}_2\text{-YF}_3$ ceramics is shown in Fig. 9 inset. The laser wavelength was located at 1049 nm with the full width at half maximum (FWHM) of 1.82 nm.

4. Conclusions

It was found that Y^{3+} ions were successfully incorporated into the Yb^{3+} : CaF_2 host even the concentration of Y^{3+} ions reached 6 at.%. Doping with Y^{3+} ions increased the lattice parameter of CaF_2 and decreased the particles size of the powders. The detailed spectral properties analysis confirmed that the optimal concentration of Y^{3+} in Yb^{3+} : CaF_2 was 1 at.%. To the best of our knowledge, laser output at the wavelength of 1049 nm was demonstrated in 3 at.% Yb, 1 at.% Y: CaF_2 transparent ceramics for the first time. A maximum output power of 1.16 W with slope efficiency of 29.3% was obtained under 978 nm LD pumping. It can be concluded that the hot-pressed method is another efficiency method to obtain laser-quality Yb^{3+} : CaF_2 transparent ceramics except HIP method.

Declaration of competing interest

The authors declare that they have no known competing financial interests or personal relationships that could have appeared to influence the work reported in this paper.

Acknowledgments

This work was supported by the National Natural Science Foundation of China (Grant Nos. 51902234, 11974220, 61635012), the Fundamental Research Funds for the Central Universities of China (WUT: 2019IVA065, 203243002, 2019-YB-011), State Key Laboratory of Advanced Technology for Materials Synthesis and Processing (Wuhan University of Technology, China) grant number: 2020-KF-16 and National Key R&D Program of China (Grant No. 2017YFB0310503).

References

- [1] A. Ikesue, Y.L. Aung, Ceramic laser materials, *Nat. Photon.* 2 (2008) 721–727.
- [2] Q. Yao, L. Zhang, J. Zhang, Z.G. Jiang, B.H. Sun, C. Shao, Y.L. Ma, T.Y. Zhou, K.G. Wang, L. Zhang, H. Chen, Y. Wang, Simple mass-preparation and enhanced thermal performance of Ce: YAG transparent ceramics for high power white LEDs, *Ceram. Int.* 45 (5) (2019) 6356–6362.
- [3] M. Siebold, S. Bock, U. Schramm, B. Xu, J.L. Doualan, P. Camy, R. Moncorge, Yb: CaF₂-a new old laser crystal, *Appl. Phys. B* 97 (2009) 327–338.
- [4] F. Druon, S. Ricaud, D.N. Papadopoulos, A. Pellegrina, P. Camy, J.L. Doualan, R. Moncorge, A. Courjaud, E. Mottay, P. Georges, On Yb: CaF₂ and Yb: SrF₂: review of spectroscopic and thermal properties and their impact on femtosecond and high power laser performance, *Opt. Mater. Express* 1 (2011) 489–502.
- [5] A. Lucca, G. Debourg, M. Jacquement, F. Druon, F. Balembois, P. Georges, High power diode-pumped Yb³⁺: CaF₂ femtosecond laser, *Opt. Lett.* 29 (2004) 2767–2769.
- [6] S. Ricaud, D.N. Papadopoulos, A. Pellegrina, F. Balembois, P. Georges, A. Courjaud, P. Camy, J.L. Doualan, R. Moncorge, F. Druon, High-power diode-pumped cryogenically cooled Yb: CaF₂ laser with extremely low quantum defect, *Opt. Lett.* 36 (2011) 1602–1604.
- [7] M. Siebold, M. Hornung, R. Boedefeld, S. Podleska, S. Klingebiel, C. Wandt, F. Krausz, S. Karsch, R. Uecker, A. Jochmann, J. Hein, M.C. Kaluza, Terawatt diode-pumped Yb: CaF₂ laser, *Opt. Lett.* 33 (2008) 2770–2772.
- [8] Y.Q. Wu, L.B. Su, Q.G. Wang, H.J. Li, Y.Y. Zhan, D.P. Jiang, X.B. Qian, C.Y. Wang, L.H. Zheng, H.B. Chen, J. Xu, W. Ryba-Romanowski, P. Solarz, R. Lisiecki, Spectroscopic properties of Yb-doped CaF₂-YF₃ solid-solution laser crystal, *Laser Phys.* 2 (2013) 105805.
- [9] H.T. Zhu, J. Liu, L.B. Su, D.P. Jiang, X.B. Qian, J. Xu, Picosecond pulse generation from a Yb: CaF₂-YF₃ mode-locked laser, *Laser Phys.* 25 (4) (2015) 045801.
- [10] Y.Y. Ren, C. Chen, Y.C. Jia, Y. Jiao, D.W. Li, M.D. Mackenzie, A.K. Kar, F. Chen, Switchable single-dual-wavelength Yb, Na: CaF₂ waveguide lasers operating in continuous-wave and pulsed regimes, *Opt. Mater. Express* 8 (6) (2018) 1633–1641.
- [11] A. Pugzlys, G. Andriukaitis, D. Sidorov, A. Irshad, A. Baltuska, W.J. Lai, P.B. Phua, L. Su, J. Xu, H. Li, R. Li, S. Alisaukas, A. Marcinkevicius, M.E. Fermann, L. Giniunas, R. Danielius, Spectroscopy and lasing of cryogenically cooled Yb, Na: CaF₂, *Appl. Phys. B* 97 (2009) 339–350.
- [12] L.B. Su, J. Xu, H.J. Li, L. Wen, Y.Q. Zhu, Z.W. Zhao, Y.J. Dong, G.Q. Zhou, J.L. Si, Sites structure and spectroscopic properties of Yb-doped and Yb, Na-codoped CaF₂ laser crystals, *Chem. Phys. Lett.* 406 (2005) 254–258.
- [13] S. Kitajima, K. Yamakado, A. Shirakawa, K.-I. Ueda, Y. Ezura, H. Ishizawa, Yb³⁺-doped CaF₂-LaF₃ ceramics laser, *Opt. Lett.* 42 (9) (2017) 1724–1727.
- [14] J. Liu, P. Liu, J. Wang, X.D. Xu, D.Z. Li, J. Zhang, X.M. Nie, Fabrication and sintering behavior of Er: SrF₂ transparent ceramics using chemically derived powder, *Materials* 11 (2018) 475.
- [15] J.L. Li, X.Q. Chen, L.F. Tang, Y.Y. Li, Y.Q. Wu, Fabrication and properties of transparent Nd-doped BaF₂ ceramics, *J. Am. Ceram. Soc.* 102 (2019) 178–184.
- [16] X.Q. Chen, Y.Q. Wu, High concentration Ce³⁺ doped BaF₂ transparent ceramics, *J. Alloys Compd.* 817 (2020) 153075.
- [17] G.Q. Yi, W.W. Li, J.H. Song, B.C. Mei, Z.W. Zhou, L.B. Su, Preparation and characterization of Pr³⁺: CaF₂ transparent ceramics with different doping concentrations, *Ceram. Int.* 45 (2019) 3541–3546.
- [18] S.E. Hatch, W.F. Parsons, R.J. Weagley, Hot-pressed polycrystalline CaF₂: Dy²⁺ laser, *Appl. Phys. Lett.* 5 (1964) 153–154.
- [19] M. Sh Akchurin, T.T. Basiev, A.A. Demidenko, M.E. Doroshenko, P.P. Fedorov, E.A. Garibin, P.E. Gusev, Kuznetsov, M.A. Krutov, I.A. Mironov, V.V. Osiko, P.A. Popov, CaF₂: Yb laser ceramics, *Opt. Mater.* 35 (2013) 444–450.
- [20] W.W. Li, H.J. Huang, B.C. Mei, J.H. Song, X.D. Xu, Effect of Y³⁺ ion doping on the microstructure, transmittance and thermal properties of CaF₂ transparent ceramics, *J. Alloys Compd.* 747 (2018) 359–365.
- [21] G.K. Williamson, W.H. Hall, X-ray line broadening from filed aluminium and wolfram, *Acta Metall.* 1 (1953) 22–31.
- [22] A.K. Bedyal, D.D. Ramteke, Vinay Kumar, H.C. Swart, Excitation wavelength and Eu³⁺/Tb³⁺ content radio dependent tunable photoluminescence from NaSrBO₃: Eu³⁺/Tb³⁺ phosphor, *J. Mater. Sci. Mater. Electron.* 30 (2019) 11714–11726.
- [23] L.L. Dong, M.Z. Ma, W. Jing, T. Xu, B. Kang, R.S. Guo, Synthesis of highly sinterable Yb: Lu₂O₃ nanopowders via spray coprecipitation for transparent ceramics, *Ceram. Int.* 45 (15) (2019) 19554–19561.
- [24] J.S. Li, Q.L. Guan, L. Liu, J.J. Yue, X.D. Li, X.D. Sun, X.W. Qi, Influence of Yb and Si on the fabrication of Yb: YAG transparent ceramics using spherical Y₂O₃ powders, *Ceram. Int.* 45 (14) (2019) 17354–17362.
- [25] F.F. Malyavin, V.A. Tarala, S.V. Kuznetsov, A.A. Kravtsov, I.S. Chikulina, M.S. Shama, E.V. Medyanik, V.S. Ziryakov, E.A. Evtushenko, D.S. Vokalov, V.A. Lapin, D.S. Kuleshov, L.V. Tarala, L.M. Mitrofanenko, Influence of the ceramic powder morphology and forming conditions on the optical transmittance of YAG: Yb ceramics, *Ceram. Int.* 45 (2019) 4418–4423.
- [26] M.I. Mendelson, Average grain size in polycrystalline ceramics, *J. Am. Ceram. Soc.* 52 (1969) 443–446.
- [27] H. Chen, A. Ikesue, H. Noto, H. Uehara, Y. Hishinuma, T. Muroga, R. Yasuhara, Nd³⁺-activated CaF₂ ceramics laser, *Opt. Lett.* 44 (13) (2019) 3378–3381.